A robust mode of climate variability in the Arctic: The Barents Oscillation

Hans W. Chen,[1,2] Qiong Zhang,[2,3] Heiner Körnich,[2,4] and Deliang Chen[5]

Received 18 April 2013; accepted 9 May 2013; published 10 June 2013.

[1] The Barents Oscillation (BO) is an anomalous wintertime atmospheric circulation pattern in the Northern Hemisphere that has been linked to the meridional flow over the Nordic Seas. There are speculations that the BO has important implications for the Arctic climate; however, it has also been suggested that the pattern is an artifact of Empirical Orthogonal Function (EOF) analysis due to an eastward shift of the Arctic Oscillation/North Atlantic Oscillation (AO/NAO). In this study, EOF analyses are performed to show that a robust pattern resembling the BO can be found during different time periods, even when the AO/NAO is relatively stationary. This "BO" has a high and stable temporal correlation with the geostrophic zonal wind over the Barents Sea, while the contribution from the AO/NAO is small. The surface air temperature anomalies over the Barents Sea are closely associated with this mode of climate variability. **Citation:** Chen, H. W., Q. Zhang, H. Körnich, and D. Chen (2013), A robust mode of climate variability in the Arctic: The Barents Oscillation, *Geophys. Res. Lett.*, *40*, 2856–2861, doi:10.1002/grl.50551.

1. Introduction

[2] Dramatic changes in the Arctic climate have been observed in recent decades, including rising surface air temperature (SAT) with a trend of up to 2°C per decade in spring [*Rigor et al*., 2000] and substantial loss of sea ice [e.g., *Cavalieri*, 2003]. These trends are often seen as an amplified response to global warming and can largely be explained by the anthropogenic forcing [*Johannessen et al*., 2004]. However, the Arctic climate system also exhibits a strong internal variability, which is largely caused by natural factors. There is, for example, evidence that the large Arctic warming in the early twentieth century was caused by natural climate variability [*Johannessen et al*., 2004; *Bengtsson et al*., 2004].

[3] The Barents Sea has been pointed out as a key region in the Arctic climate system. *Goosse and Holland* [2005] found that the meridional heat exchange between the North Atlantic and Arctic sector has a predominate role in driving the natural Arctic climate variability in the Community Climate System Model. Changes in the oceanic and atmospheric heat transport into the Barents Sea were particularly important in the model simulations. The heat transport in the ocean is connected to changes in the atmospheric circulation, since the inflow of warm Atlantic water into the Barents Sea is largely driven by the wind stress.

[4] In *Bengtsson et al*. [2004], the large Arctic warming in the early twentieth century was explained by enhanced westerly winds between Spitsbergen and Norway. This led to an increased oceanic heat transport into the Barents Sea and a subsequent retreat of sea ice in this region. The mechanism for sustaining the wind anomalies was described as a positive feedback loop, where an anomalous cyclonic circulation was created over the Barents Sea by enhanced surface heat fluxes due to the sea ice loss, thus driving more warm water into the Barents Sea.

[5] *Goosse and Holland* [2005] and *Bengtsson et al*. [2004] examined the relationship between changes in Arctic climate conditions and the Arctic Oscillation/North Atlantic Oscillation (AO/NAO), but found that it was not robust over longer time periods. Both studies remarked that there were similarities with another mode of climate variability called the Barents Oscillation (BO). The BO was originally found as the second Empirical Orthogonal Function (EOF) of monthly sea level pressure (SLP) anomalies northward of 30°N for the winter months December through March (DJFM) [*Skeie*, 2000]. With a primary center of action located over the Barents Region, the BO is related to the meridional flow over the Nordic Seas and sensible heat loss in the same region. *Skeie* [2000] noted that the BO could not be found during the period 1899–1947, although it could not be concluded whether this was because of a change in the atmospheric circulation or due to poor data coverage.

[6] *Tremblay* [2001] offered a different interpretation of the BO and suggested that it cannot be considered a robust and physical mode of variability. Using a toy model, it was shown that a BO-like pattern can arise from the EOF analysis due to a shift in the action centers of the leading mode, the AO [*Thompson and Wallace*, 1998]. Thus, the BO could be a manifestation of nonstationarity in the AO pattern, in particular the large eastward shift of the AO action centers in the mid-seventies [e.g., *Hilmer and Jung*, 2000]. Although the AO and BO are unrelated over the whole time period by construction, *Tremblay* [2001] showed that their principal components (PCs) are negatively correlated ($r = -0.29$) over the period 1949–1976 and positively correlated ($r = 0.40$) for 1977–1999. This result resembles the toy model where the first two PCs are perfectly anticorrelated before the shift and perfectly correlated after the shift, resulting in zero

[1]Department of Meteorology, The Pennsylvania State University, University Park, Pennsylvania, USA.
[2]Formerly at Department of Meteorology, Stockholm University, Stockholm, Sweden.
[3]Department of Physical Geography and Quaternary Geology, Stockholm University, Stockholm, Sweden.
[4]Swedish Meteorological and Hydrological Institute, Norrköping, Sweden.
[5]Department of Earth Sciences, University of Gothenburg, Gothenburg, Sweden.

Corresponding author: D. Chen, Department of Earth Sciences, University of Gothenburg, Guldhedsgatan 5A, Box 460, 405 30 Gothenburg, Sweden. (deliang@gvc.gu.se)

0094-8276/13/10.1002/grl.50551

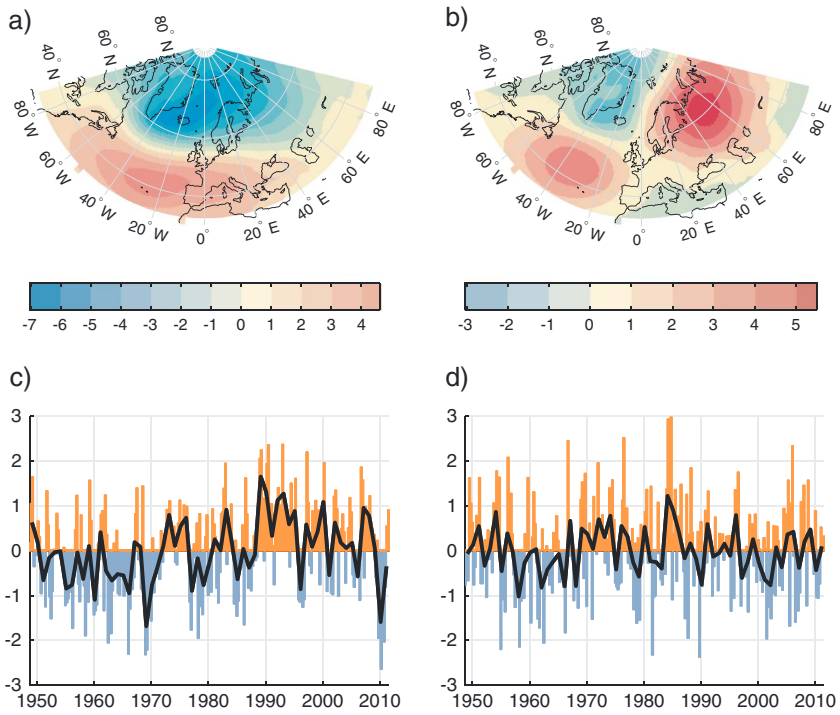

Figure 1. First and second EOFs of monthly wintertime (DJFM) SLP anomalies (hPa) in the selected region from 1949 to 2011 and their corresponding PCs. The patterns associated with the (a) North Atlantic Oscillation and (b) Barents Oscillation and (c, d) their time-varying index. The black line in Figures 1c and 1d is the annual mean.

correlation over the whole time period. Their study also pointed out that the BO pattern could not be found in the first four EOFs in the second time period (1977–1999).

[7] Recent rapid shifts of atmospheric circulations in the Northern Hemisphere [e.g., *Zhang et al*., 2008] have led to an increasing interest in studying circulation patterns other than the traditionally dominant wintertime modes, the AO/NAO and Pacific/North American pattern (PNA) [e.g., *Quadrelli and Wallace*, 2004]. *Overland and Wang* [2005] showed that the Arctic climate can be controlled by EOFs other than the first two corresponding to the AO and PNA. They found that a meridional BO-like pattern, defined as the third EOF of SLP anomalies north of 20°N, had a larger influence on SLP during spring 2000–2005 than the AO and PNA combined. The BO-like mode plays an important role in contributing to the meridional dipole pattern over the Arctic and was referred to as the Arctic Dipole by *Overland and Wang* [2010]. A large number of recent studies have shown that the more meridional atmospheric circulation contributed to dramatic loss of sea ice in the Arctic [e.g., *Overland et al*., 2008; *Zhang et al*., 2008; *Overland and Wang*, 2010] and anomalously cold winters in Eurasia [*Honda et al*., 2009; *Overland et al*., 2011]. However, it remains to show that the BO (or Arctic Dipole) is independent of the AO/NAO and not due to the nonstationarity of the leading mode, as suggested by *Tremblay* [2001].

[8] The purpose of this study was to investigate if the BO is a robust, independent mode of climate variability and further examine its implications for the Arctic climate, particularly in the Barents Sea region. To do this, we performed multiple EOF analyses over different time periods covering both recent decades and the early twentieth century. An objective circulation classification system was used to link the BO to the atmospheric circulation over the Barents Sea, independent of the EOF analysis. Finally, we took a closer look at the relationship between the BO and the SAT anomalies over the Barents Sea.

2. Data and Methods

[9] Two reanalysis data sets were used in this study, National Centers for Environmental Prediction (NCEP) and National Center for Atmospheric Research (NCAR) Reanalysis 1 (NCEP R1) [*Kalnay et al*., 1996] from 1948 to 2011, and National Oceanic and Atmospheric Administration (NOAA) Twentieth Century Reanalysis (20CR) [*Compo et al*., 2011] spanning 1871–2010. The horizontal resolution of NCEP R1 is 2.5° × 2.5° for SLP and 1.9° × 1.9° for 2 m SAT data, while 20CR has a resolution of 2.0° × 2.0°.

[10] Monthly wintertime (DJFM) SLP anomalies were decomposed using area-weighted EOFs in a region over the North Atlantic and Arctic sector (90°W–90°E and northward of 30°N). This differs from the method of *Skeie* [2000] and *Tremblay* [2001], which used the full latitude circle. The main purpose of the limited region is to exclude SLP variability over the Pacific Ocean and North America associated with the prominent PNA. All EOFs and PCs in this study have been scaled by the standard deviation of the PC, so that the EOF patterns show the variation associated with one positive standard deviation of the corresponding PC time series.

[11] Following the method used by *Chen* [2000], we applied an objective circulation classification on monthly SLP over the Barents Sea from the NCEP R1 data set. The analysis area was defined from latitudes 65°N to 85°N and longitudes 22.5°E to 52.5°E, with a grid spacing of 5° latitude by 10° longitude. Six circulation indices were obtained, describing the zonal and meridional components of geostrophic wind and

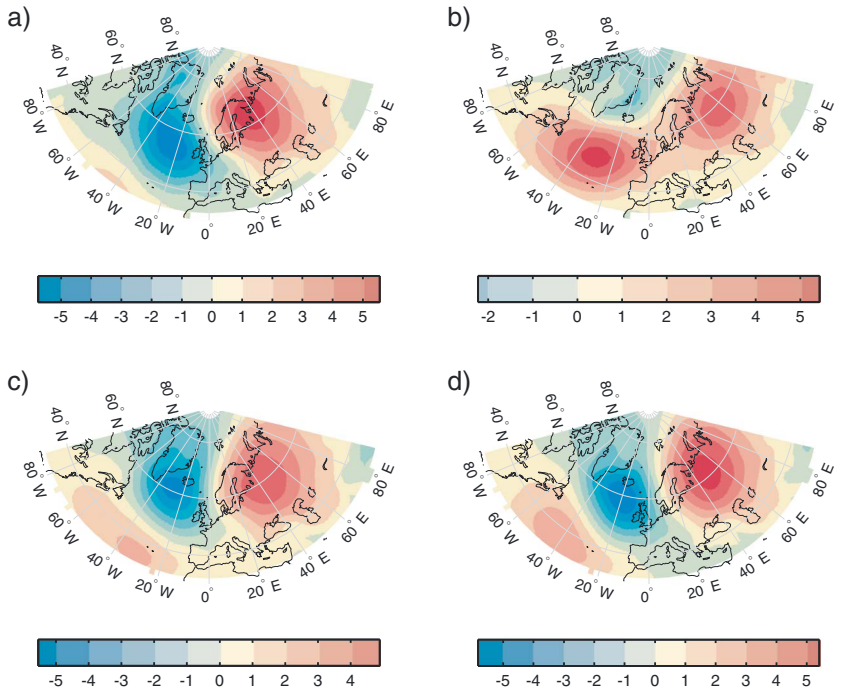

Figure 2. EOF 2 of SLP anomalies (hPa) over different sub-periods, using monthly SLP data in the winter season (DJFM) from NCEP R1 (a and b) and 20CR (c and d). (a) 1949–1976, (b) 1977–2011, (c) 1872–1909, and (d) 1910–1948.

shear vorticity, total wind speed, and total shear vorticity in the region of interest. We then examined the relationship between the indices and the temporal variation of the leading EOFs. See *Chen* [2000] for a more thorough explanation of the classification system.

3. Results

[12] The first two EOFs of monthly wintertime SLP anomalies from NCEP R1, 1949–2011, are shown in Figure 1. EOF 1 reflects the large-scale NAO pattern with the Azores high and Icelandic low pressure centers. It accounts for 33.5% of the total variance in the selected domain and is well separated from the other modes according to North's rule of thumb [*North et al*., 1982].

[13] EOF 2 (Figure 1b) has its primary center of action over the Barents Region, with another action center located over the North Atlantic Ocean and a center with opposite sign over Greenland. The pattern differs slightly from the one found by *Skeie* [2000, Figure 1b], mainly in that it has another positive center over the North Atlantic Ocean. However, the pattern is sufficiently similar and we will henceforth refer to it as the Barents Oscillation (BO).

[14] The BO in the limited region closely corresponds to the hemispheric EOF 3 (temporal correlation $r = 0.94$) and has similar centers of action as the Arctic Dipole [*Overland and Wang*, 2005, 2010; *Overland et al*., 2008]. In the smaller domain, EOF 2 explains 15.1% of the SLP variability and is not well separated from EOF 3 (14.2%), which means that they may be mixed due to sampling errors [*North et al*., 1982]. Therefore, it is important to investigate if the pattern can be reproduced reliably. PC 2 displays a large intraseasonal and interannual variability with no obvious long-term trend, see Figure 1d.

[15] *Tremblay* [2001] attributed the BO (their EOF 3) to a shift in the action center locations of EOF 1 around 1976. Following their study, we divided the period into two sub-periods, 1949–1976 and 1977–2011, and performed an EOF analysis on each sub-period. The results reveal an apparent eastward shift of the first EOF between 1949–1976 and 1977–2011. However, a BO-like pattern is still found in EOF 2 in the two sub-periods, as shown in Figure 2. (The change in the spatial pattern may be related to the recent changes in the atmospheric circulation patterns [e.g., *Zhang et al*., 2008], but the exact reason behind the change and its implications are beyond the scope of this study.) This result contrasts with the findings of *Tremblay* [2001], who did not find the BO in the first four EOFs in their second sub-period. Repeating the analysis with the same years as *Tremblay* [2001] (1977–1999) did not change the results significantly; the obtained EOF 2 looks similar to the one in Figure 2b but with slightly shifted centers. Thus, the reason for the disparate results is likely due to how the domain is chosen for the EOF analysis. By limiting the longitude range in this study to between 90°W and 90°E, the large SLP variability associated with the PNA is no longer taken into consideration when constructing the EOFs, which leads to a more robust pattern in EOF 2.

[16] The second EOF explains 18.2% of the total variance in the first sub-period (Figure 2a) and 15.7% in the second period (Figure 2b). The most prominent difference between the spatial patterns in the two sub-periods is the large negative center in Figure 2a. During 1977–2011, the center is much weaker and restricted to north of 60°N. A likely explanation is poor separation between the EOFs. In the second sub-period (1977–2011), the fourth EOF displays a similar negative center over the North Atlantic Ocean as Figure 2a. The center over the Barents Region, however, appears to be stable in both sub-periods.

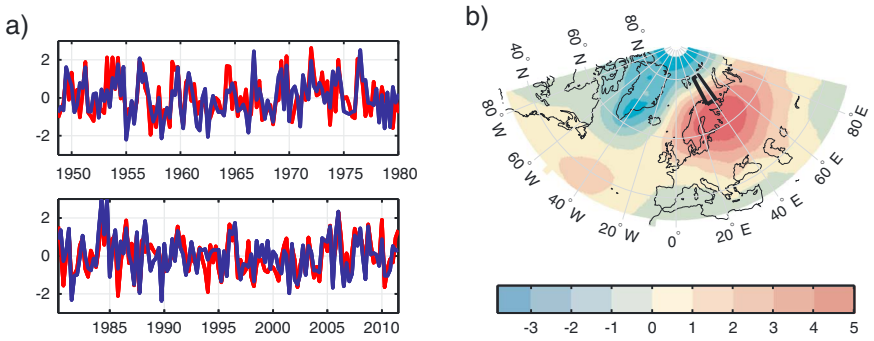

Figure 3. (a) Standardized PC 2 (blue) and geostrophic zonal wind U over the Barents Sea (red) during the winter season (DJFM). The time series is continuous but has been divided into two parts for viewing clarity. (b) Linear regression of wintertime SLP anomalies on standardized U during 1949–2011. The map shows the SLP variations associated with one positive standard deviation of U. The region where U was calculated is indicated with a black box.

[17] To further test the robustness of the second EOF, the analyses were repeated using early twentieth century SLP data from 20CR. Figures 2c and 2d show the second EOFs for the sub-periods 1872–1909 and 1910–1948, which account for 20.7% and 18.2% of the explained variance in respective period. The EOF 2 patterns from 20CR show similar centers of action as the second EOF from NCEP R1 (see, e.g., Figure 2a) and support our BO pattern. We also performed EOF analyses on observational SLP data from NCAR Northern Hemisphere Sea-Level Pressure (NCAR SLP) [*Trenberth and Paolino*, 1980] and Hadley Centre Sea Level Pressure (HadSLP2) [*Allan and Ansell*, 2006]. In contrast to *Skeie* [2000], who could not find the BO during 1899–1947 when using the NCAR SLP data set, we find a similar EOF 2 pattern as the ones from 20CR (Figures 2c and 2d) in NCAR SLP during 1872–1947 and 1949–2011, as well as during 1851–1948 and 1949–2004 in HadSLP2 (not shown). This gives us further confidence that the BO is a stable mode of climate variability.

[18] PC 2, associated with the BO pattern, shows a strong correlation ($r = 0.71$) with the geostrophic zonal wind U over the Barents Sea, which is one of the six circulation indices obtained from the objective classification for the period 1949–2011 (see *Chen* [2000] for more information). The standardized time series of PC 2 and U are shown in Figure 3a. It appears that the relation between PC 2 and U is high during the whole period. A regression analysis of SLP anomalies in NCEP R1 on U reveals a pattern strikingly similar to EOF 2 from the same period, compare Figure 3b with 1b. Similar regression patterns were found when dividing the analysis period into two sub-periods, 1949–1976 and 1977–2011. The results still resemble the BO when SLP anomalies associated with the NAO were removed.

[19] The correlation between U and PC 1 is weak over the whole period, −0.12. In order to test whether the regime shift of the NAO in the mid-seventies has any impact on the relation between U and the NAO/BO, we used the earlier EOF analyses for 1949–1976 and 1977–2011 to calculate the correlation between U and PC 1/PC 2 in each respective sub-period. This method is different from using the EOF analysis over the whole period and calculating a correlation coefficient for each sub-period, since a change in the EOF pattern during one period will yield a different PC.

[20] The correlation analysis shows that the linear relationship between U and PC 1 is weak in both sub-periods, 0.14 for 1949–1976 and −0.08 for 1977–2011. PC 2, on the other hand, is well related to U, with a correlation coefficient $r = 0.66$ over the period 1949–1976 and $r = 0.61$ during 1977–2011. These results indicate that the second EOF has a physical meaning and is not purely an artifact due to a shift in the leading EOF.

[21] Over the whole period, the correlation between PC 2 and the other indices from the circulation classification ranges from moderate (0.35 with the geostrophic meridional wind over the Barents Sea and −0.36 with the zonal component of vorticity) to weak. PC 1 shows only a weak correlation with all indices. The mean atmospheric circulation at the surface is dominated by cyclonic activity, 61.3% of the winter months are classified as the cyclonic (C) type. If hybrid types containing C are included, the number increases to 80.5%. An SLP composite of months classified as C minus months of other types reveals a cyclone centered over the Barents Sea (not shown).

[22] SAT anomalies associated with the BO have their largest amplitude over the Barents Sea, as shown in the regression map in Figure 4a. A positive PC 2 is associated with enhanced southerly winds over the Nordic Seas and westerly wind anomalies over the Barents Sea, which can drive an increased atmospheric and oceanic heat transport into the Barents Sea (as described by *Goosse and Holland* [2005] and *Bengtsson et al.* [2004]). There is also a significant cooling over the Labrador Sea and a large part of Eastern Europe, likely related to enhanced northerly winds.

[23] The SAT regression pattern in Figure 4a is remarkably similar to the second EOF of monthly SAT anomalies in the winter season (DJFM), shown in Figure 4b, which explains 15.1% of the total SAT variance in the whole domain. A strong correlation (0.72) is found between the SAT PC 2 and the SLP PC 2 from Figure 1d, which we will refer to as the BO index from now on to avoid confusion. It also resembles the fourth EOF of wintertime SAT anomalies found by *Semenov and Bengtsson* [2003]. Similarly, the first EOF of SAT anomalies (23.3% of the explained variance, not shown) is associated with the NAO and has a 0.84 correlation with the SLP PC 1.

[24] The BO index is generally well related to the horizontally averaged SAT anomalies over the Barents Sea, defined as the domain within 70°N–80°N latitude and 0°E–60°E longitude. During 1949–1989, the temporal correlation between the two is 0.65. However, between 1990 and 2003,

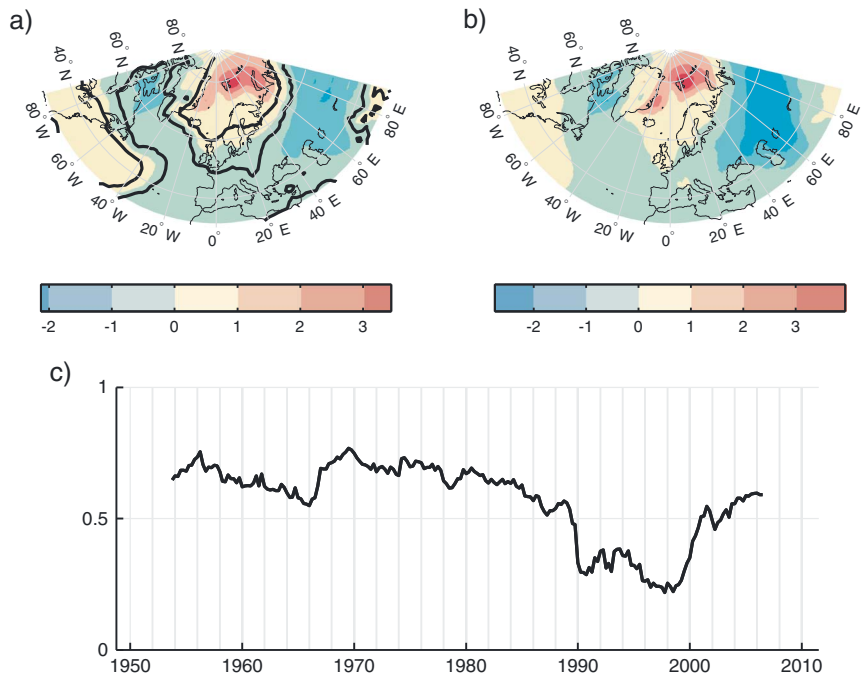

Figure 4. (a) Linear regression of winter SAT anomalies (°C) on SLP PC 2. Regions within contours are statistically significant at the 95 % confidence level. (b) Second EOF of monthly wintertime SAT anomalies (°C). (c) Moving correlation between SAT anomalies over the Barents Sea and SLP PC 2, with a time window of 33 months (about 8 years).

the correlation suddenly decreases to 0.26, then increases to 0.66 for 2004–2011. The correlation over the whole period is 0.52. Figure 4c shows the sudden dip in the correlation around 1990. A similar result is found when substituting the BO index with U or SAT PC 2 in the correlation analysis. The results suggest that none of the variables alone can adequately explain the SAT variability over the Barents Sea during the 1990–2003 period. The reason for this result still remains an open question.

[25] *Skeie* [2000] mentioned that the BO is similar to another teleconnection pattern called the Scandinavia Pattern (SCAND), which was first introduced by *Barnston and Livezey* [1987] (referred to as Eurasian pattern Type 1). The temporal correlation between the BO index and SCAND index, obtained from NOAA/Climate Prediction Center, is 0.66 for 1949–2011 during the winter months (DJFM). The BO is better related to the geostrophic zonal wind over the Barents Sea ($r = 0.71$, compared to 0.60 for SCAND) and may thus better describe the mode that is important for the Arctic climate variability.

4. Concluding Remarks

[26] This study shows that the BO is a stable mode that can be found during four sub-periods from 1872 to 2011. It is not well separated from EOF 3; however, the pattern could be reproduced over various time periods and in different reanalysis and observational data sets.

[27] We restricted the EOF analysis region to the North Atlantic and Arctic sector to obtain a more robust BO pattern. When doing an EOF analysis over the full latitude circle, the second EOF usually corresponds to the PNA [*Quadrelli and Wallace*, 2004]. Excluding most of the SLP variability over the Pacific Ocean and North America associated with the PNA resulted in a better separation of the EOFs. Thus, we were able to identify the BO during 1977–1999 while *Tremblay* [2001] could not find it for the same time period. Contrary to the results of *Skeie* [2000], the BO could also be found in the NCAR SLP data set for 1899–1947. Surprisingly the NCAR SLP result from this study was not sensitive to the analysis region; the BO could still be obtained when not restricting the longitude range. However, it appeared as EOF 2 (which usually represents the PNA) instead of EOF 3 during 1899–1947. In the later time period (1949–2011), the BO was found as the hemispheric EOF 3 in NCAR SLP. One possible explanation for this discrepancy is that *Skeie* [2000] used a slightly different method when doing the EOF analysis. It could also explain why the BO was originally found as EOF 2, while subsequent studies (including this one for the hemispheric EOF analysis) found it as EOF 3 [*Tremblay*, 2001; *Overland and Wang*, 2005; *Overland et al*., 2008; *Overland and Wang*, 2010].

[28] In the correlation analyses with the geostrophic zonal wind U over the Barents Sea, we divided the time period into two sub-periods around when the shift in the AO/NAO occurred. PC 2 still shows a high correlation with U, while the correlation between PC 1 and U is weak in both sub-periods. The regression of SLP anomalies on U also supports the BO pattern. Although we cannot exclude that some variability in EOF 2 is related to the nonstationarity of the AO/NAO, this result strongly suggests that the BO is an independent mode of the AO/NAO.

[29] Even though the large-scale NAO pattern explains a larger amount of the total SLP variance than the second EOF, it mostly modulates SAT in the zonal direction. Therefore, a regional pattern like the BO may be more important for the Arctic climate conditions. Indeed, the BO is well related to the meridional flow over the Nordic Seas and zonal wind anomalies over the Barents Sea, both of which have been found to be important for driving the natural Arctic

SAT variability in previous studies. A positive BO index is associated with a warming in the Arctic, particularly over the Barents Sea. We can also confirm the linkage between the BO and sensible heat loss over the Barents Sea (first identified by *Skeie* [2000]) using 20CR data.

[30] Here we have focused on the physical interpretation of the BO and did not investigate the mechanisms behind it. Previous observational and modeling studies have linked recent loss of Arctic sea ice in summer to a more meridional atmospheric circulation pattern in winter, changes in cyclone tracks, anomalously cold Eurasian winters, and more rapid decline of sea ice extent in the Arctic [e.g., *Inoue et al*., 2012; *Honda et al*., 2009; *Hopsch et al*., 2012; *Overland and Wang*, 2010; *Overland et al*., 2008, 2011; *Petoukhov and Semenov*, 2010]. In the study by *Honda et al*. [2009], they found a circulation pattern in November with a primary center over the Barents Region associated with decreased Arctic sea ice in early autumn. The related SAT pattern shows a warm Arctic-cold Eurasian continent dipole, reminiscent of the SAT regression pattern associated with the BO (Figure 4a). *Honda et al*. [2009] explained the mechanism as a stationarity Rossby wave generated around the Barents-Kara Seas by the anomalous sensible and latent heat fluxes due to reduced sea ice cover. Whether this is related to the BO still remains to be studied.

[31] EOF analysis has many limitations, for example, the spatial patterns are assumed to be either stationary or propagating, and the EOFs are forced to be orthogonal to each other. There are similar methods that try to overcome these limitations such as rotated EOF, but they usually have their own shortcomings. In this study, the EOF 2 patterns were verified using regression analysis. We have shown that the second EOF of wintertime SLP anomalies over the North Atlantic and Arctic sector has a physical meaning and that it has consequences for the SAT variability over the Barents Sea. Whether by EOF analysis or by using other methods, this mode of climate variability is worth investigating further.

[32] **Acknowledgments.** This work was supported by the Bert Bolin Centre for Climate Research at Stockholm University. The authors thank Tinghai Ou and Léon Chafik for valuable discussions, and two anonymous reviewers for their helpful suggestions. NCEP R1 and HadSLP2 data were provided by the NOAA/OAR/ESRL PSD, Boulder, Colorado, USA, from their website at http://www.esrl.noaa.gov/psd/. Support for the 20CR data set is provided by the U.S. Department of Energy, Office of Science Innovative and Novel Computational Impact on Theory and Experiment (DOE INCITE) program, and Office of Biological and Environmental Research (BER), and by the National Oceanic and Atmospheric Administration Climate Program Office.

[33] The Editor thanks two anonymous reviewers for their assistance in evaluating this paper.

References

Allan, R., and T. Ansell (2006), A new globally complete monthly historical gridded mean sea level pressure data set (HadSLP2): 1850–2004, *J. Climate*, *19*(22), 5816–5842, doi:10.1175/JCLI3937.1.

Barnston, A. G., and R. E. Livezey (1987), Classification, seasonality and persistence of low-frequency atmospheric circulation patterns, *Mon. Weather Rev.*, *115*(6), 1083–1126, doi:10.1175/1520-0493(1987)115<1083:CSAPOL>2.0.CO;2.

Bengtsson, L., V. A. Semenov, and O. M. Johannessen (2004), The early twentieth-century warming in the Arctic—A possible mechanism, *J. Climate*, *17*, 4045–4057, doi:10.1175/1520-0442(2004)017<4045:TETWIT>2.0.CO;2.

Cavalieri, D. J. (2003), 30-year satellite record reveals contrasting Arctic and Antarctic decadal sea ice variability, *Geophys. Res. Lett.*, *30*(18), 1970, doi:10.1029/2003GL018031.

Chen, D. (2000), A monthly circulation climatology for Sweden and its application to a winter temperature case study, *Int. J. Climatol.*, *20*(10), 1067–1076.

Compo, G. P., et al. (2011), The twentieth century reanalysis project, *Q. J. Roy. Meteorol. Soc.*, *137*(654), 1–28, doi:10.1002/qj.776.

Goosse, H., and M. M. Holland (2005), Mechanisms of decadal Arctic climate variability in the Community Climate System Model, Version 2 (CCSM2), *J. Climate*, *18*(17), 3552–3570, doi:10.1175/JCLI3476.1.

Hilmer, M., and T. Jung (2000), Evidence for a recent change in the link between the North Atlantic Oscillation and Arctic sea ice export, *Geophys. Res. Lett.*, *27*(7), 989–992, doi:10.1029/1999GL010944.

Honda, M., J. Inoue, and S. Yamane (2009), Influence of low Arctic sea-ice minima on anomalously cold Eurasian winters, *Geophys. Res. Lett.*, *36*, L08707, doi:10.1029/2008GL037079.

Hopsch, S., J. Cohen, and K. Dethloff (2012), Analysis of a link between fall Arctic sea ice concentration and atmospheric patterns in the following winter, *Tellus Ser. A*, *64*, doi:10.3402/tellusa.v64i0.18624.

Inoue, J., M. E. Hori, and K. Takaya (2012), The role of Barents Sea ice in the wintertime cyclone track and emergence of a warm-Arctic cold-Siberian anomaly, *J. Climate*, *25*(7), 2561–2568, doi:10.1175/JCLI-D-11-00449.1, WOS:000302142800027.

Johannessen, O. M., et al. (2004), Arctic climate change: Observed and modelled temperature and sea-ice variability, *Tellus A*, *56*(4), 328–341, doi:10.1111/j.1600-0870.2004.00060.x.

Kalnay, E., et al. (1996), The NCEP/NCAR 40-year reanalysis project, *Bull. Am. Meteorol. Soc.*, *77*(3), 437–471, doi:10.1175/1520-0477(1996)077<0437:TNYRP>2.0.CO;2.

North, G. R., T. L. Bell, R. F. Cahalan, and F. J. Moeng (1982), Sampling errors in the estimation of Empirical Orthogonal Functions, *Mon. Weather Rev.*, *110*(7), 699–706, doi:10.1175/1520-0493(1982)110<0699:SEITEO>2.0.CO;2.

Overland, J. E., and M. Wang (2005), The third Arctic climate pattern: 1930s and early 2000s, *Geophys. Res. Lett.*, *32*(23), L23808, doi:10.1029/2005GL024254.

Overland, J. E., and M. Wang (2010), Large-scale atmospheric circulation changes are associated with the recent loss of Arctic sea ice, *Tellus Ser. A*, *62*(1), 1–9, doi:10.1111/j.1600-0870.2009.00421.x.

Overland, J. E., M. Wang, and S. Salo (2008), The recent Arctic warm period, *Tellus A*, *60*(4), 589–597, doi:10.1111/j.1600-0870.2008.00327.x.

Overland, J. E., K. R. Wood, and M. Wang (2011), Warm Arctic-cold continents: Climate impacts of the newly open Arctic sea, *Polar Res.*, *30*(0), doi:10.3402/polar.v30i0.15787.

Petoukhov, V., and V. A. Semenov (2010), A link between reduced Barents-Kara sea ice and cold winter extremes over northern continents, *J. Geophys. Res.*, *115*, D21111, doi:10.1029/2009JD013568.

Quadrelli, R., and J. M. Wallace (2004), A simplified linear framework for interpreting patterns of Northern Hemisphere wintertime climate variability, *J. Climate*, *17*(19), 3728–3744, doi:10.1175/1520-0442(2004)017<3728:ASLFFI>2.0.CO;2.

Rigor, I. G., R. L. Colony, and S. Martin (2000), Variations in surface air temperature observations in the Arctic, 1979–97, *J. Climate*, *13*(5), 896–914, doi:10.1175/1520-0442(2000)013<0896:VISATO>2.0.CO;2.

Semenov, V. A., and L. Bengtsson (2003), Modes of the wintertime Arctic temperature variability, *Geophys. Res. Lett.*, *30*(15), 1781, doi:10.1029/2003GL017112.

Skeie, P. (2000), Meridional flow variability over the Nordic seas in the Arctic Oscillation framework, *Geophys. Res. Lett.*, *27*(16), 2569, doi:10.1029/2000GL011529.

Thompson, D., and J. Wallace (1998), The Arctic Oscillation signature in the wintertime geopotential height and temperature fields, *Geophys. Res. Lett.*, *25*(9), 1297–1300, doi:10.1029/98GL00950.

Tremblay, L.-B. (2001), Can we consider the Arctic Oscillation independently from the Barents Oscillation?, *Geophys. Res. Lett.*, *28*(22), 4227–4230, doi:10.1029/2000GL013740.

Trenberth, K. E., and D. A. Paolino (1980), The Northern Hemisphere sea-level pressure data set: Trends, errors and discontinuities, *Mon. Weather Rev.*, *108*(7), 855–872, doi:10.1175/1520-0493(1980)108<0855:TNHSLP>2.0.CO;2.

Zhang, X., A. Sorteberg, J. Zhang, R. Gerdes, and J. C. Comiso (2008), Recent radical shifts of atmospheric circulations and rapid changes in Arctic climate system, *Geophys. Res. Lett.*, *35*, L22701, doi:10.1029/2008GL035607.